INDERSCIENCE PUBLISHERS
Linking academia, business and industry through research

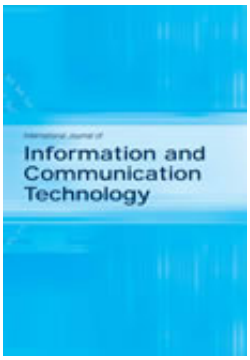

International Journal of Information and Communication Technology

ISSN online: 1741-8070 - ISSN print: 1466-6642
https://www.inderscience.com/ijict

Edge detection algorithm of insulator hydrophobic image in CPS system considering deconvolution and deblurring algorithm

Junchao Wei

Article History:

Received:	28 June 2024
Last revised:	23 August 2024
Accepted:	08 September 2024
Published online:	10 October 2024

Edge detection algorithm of insulator hydrophobic image in CPS system considering deconvolution and deblurring algorithm

Junchao Wei

Department of Basic Courses,
Xi'an Traffic Engineering Institute,
Xi'an, Shaanxi, 710300, China
Email: weijunchao@xjy.edu.cn

Abstract: Through experiments, this paper verifies the practicability and effectiveness of the deconvolution deblurring algorithm. Through fuzzy kernel estimation and sharp edge recovery, we have effectively improved the defects of traditional edge detection algorithms, which also solve the clear hydrophobic image under CPS. The experimental data show that, compared with the traditional edge detection algorithm, the comprehensive PSNR value of the edge detection algorithm of insulator hydrophobic image based on deconvolution and deblurring algorithm in CPS environment is 27.02, and the improvement range is about 0.3 dB to 1.9 dB. In terms of operation time, the average operation time of this algorithm is reduced by about two-thirds. Therefore, the following conclusions are drawn in this paper. The edge detection accuracy of insulator hydrophobic image considering deconvolution deblurring algorithm is very high, and the convergence performance is also very good.

Keywords: image edge detection algorithm; deconvolution deblurring algorithm; insulator water repellency; image processing; CPS.

Reference to this paper should be made as follows: Wei, J. (2024) 'Edge detection algorithm of insulator hydrophobic image in CPS system considering deconvolution and deblurring algorithm', *Int. J. Information and Communication Technology*, Vol. 25, No. 7, pp.1–15.

Biographical notes: Junchao Wei earned a Bachelor's in Education from Sichuan Normal University (2002–2006) and a Masters in Engineering in 2017. Since then, he has been active in teaching and research at Xi'an Traffic Engineering Institute, managing teaching in the Basic Courses Department. He also published four scholarly articles, with research interests in graphics, imaging, and computer intelligent systems.

1 Introduction

Following the mature progress of informatisation building and the expansion of power grid scale, the power system has been continuously improved. As one of the important equipment for system line insulation, insulators have attracted more and more attention to their quality and safety performance. However, as the running time goes on and on, the insulator will age in different degrees under the influence of external environmental

factors, which not only seriously affects its application value, but also easily causes accidents. Therefore, its hydrophobicity must be regularly tested. However, because of the issues of poor contrast, shadow, and uneven illumination in conventional hydrophobic image edge detection algorithms, it is difficult to obtain good results in image manipulation. Therefore, it is very urgent to build a set of efficient image edge detection algorithm to protect the safety of power grid lines. The deconvolution deblurring algorithm, as one of the image restoration technology algorithms, can not only etains the maximum amount of valuable information in the image, but also has a good image processing effect, and is widely used in the area of science and engineering. Using it in insulator detection can increase the precision of hydrophobicity measurements, and has practical value in improving the performance of the insulator hydrophobic image edge inspection algorithms.

The improvement of the performance of the edge detection algorithm for insulator hydrophobic images has always been the focus of many scholars' research. In order to investigate the causes of the hydrophobicity fluctuations of the algorithm, Cheng et al. (2018) conducted superficial energy test and FTIR spectrum analysis of the surface material according to the two-drop approach. Shaik et al. (2017) made a brief study on the edge detection algorithm of insulator hydrophobic image with noise, and found a better method by comparing the experimental results. Zhang and Zhang (2019) conducted in-depth research on the principle of edge detection algorithm for insulator hydrophobic image, and realised the accurate location and extraction of image edge. Yu et al. (2018) used the up-down method to study the pollution flashover performance of the insulator hydrophobic image edge inspection methods and the influence of the high electric field strength part. Jayabal et al. (2019) used PC analysis to rank features extracted from binary images according to their principal components, and found that edge detection algorithms improved categorisation precision with the build-up of sequential characteristics. Leng et al. (2017) conducted experiments on the edge detection algorithm of insulator hydrophobic images by incorporating Gaussian filtering and bilateral filtering. The results demonstrated that the method enables significant decrease in computational effort and obtain better performance. As the insulator inspection technology has improved, the expansion of the industry has a higher demand for algorithms. The insulator hydrophobicity under the previous research approaches has struggled to match the new needs in terms of quality and efficiency, and the deconvolution deblurring algorithm can play its advantages in this problem.

In past studies, deconvolution deblurring algorithms have been tried to deal with various image problems. Chang et al. (2017) proposed a novel single-image deconvolution deblurring algorithm for processing non-uniform movement images ambiguous by motion objects. Hang et al. (2017) developed an efficient image restoration method based on deconvolution deblurring and applied it to the image model through denoising decoupling technique. Zheng et al. (2018) proposed an modified single-image deconvolution rapid deblurring method to constrain the image gradient distribution. In order to solve the problem that the sampled fluorescence signal is distorted by optical blurring and photon counting noise, Tao et al. (2019) introduced a deconvolution deblurring method to reduce the degradation problem. Zhe et al. (2018) used the deconvolution deblurring algorithm to analyse the blurred image problem of hand-held cameras in low light conditions. Chang et al. (2018) divided the blurred image into a sharp edge portion and a flat portion, and proposed a mixed single-image motion-based deconvolution deblurring method to solve the existing issues. The deconvolution

deblurring algorithm has been well used in recent years. However, the idea of combining it with the insulator hydrophobic image edge detection algorithm to solve practical problems has not been deeply explored. To better enhance the efficiency and value of the algorithm. The edge detection algorithm of insulator hydrophobic image considering deconvolution deblurring algorithm is of great significance.

Considering the deconvolution deblurring algorithm, it further improves and enhances the defects existing in the edge detection algorithm of insulator hydrophobic image. The algorithm verification data shows that the comprehensive PSNR value of the six types of hydrophobic images under the algorithm in it is 27.02, while the traditional edge detection algorithm is 26.33, and the maximum improvement is about 1.9 dB. The RRE values of the two algorithms also show a big difference. The comprehensive value of the algorithm in it is only 6.55, while the average RRE of the traditional edge detection algorithm reaches 6.98. In terms of running time, the average operation time of it is shortened by nearly 2/3 by comparison with the conventional approach. It can be seen from the verification data that the insulator hydrophobic image edge inspection method taking into account the deconvolution and deblurring method can shorten the running time of the algorithm and ensure its feasibility on the basis of good detection results.

2 Deconstruction of image edge detection algorithm for insulator hydrophobicity

2.1 Characteristics of insulator hydrophobicity image and its algorithm processing

As a general inspection and control of insulation on overhead electricity distribution lines and atop locomotives, insulators are an important device to guarantee the correct functioning of the whole distribution line system and locomotive motive force system. Its excellent electrical properties are manifested in hydrophobicity, but the hydrophobicity of insulators is not constant. As the operating time of the insulator becomes longer, the hydrophobicity of its surface will become worse and worse.

Generally speaking, the reasons for the decrease in the hydrophobicity of insulators include five aspects, as shown in Table 1.

Table 1 Reasons for the drop in hydrophobicity of insulators

Sequence	*Reason*	*Illustrate*
1	Damp	Sharp drop in surface resistance leads to a sharp increase in leakage current
2	Contaminant composition and accumulation level	Decreased hydrophobicity due to dirt accumulation
3	Low temperature	Low temperature reduces Brownian motion of LMW molecules
4	Quality	Quality makes the difference in hydrophobicity
5	Ageing	Aging deteriorates the insulator composition

It is obvious from Table 1 that with the increase of operating time, the insulator will show different degrees of aging, and its hydrophobicity will also decrease to different degrees.

Under the current environmental reality of a vast area and a large population, the number of insulators used in power construction is also very large, and the resulting flashover accidents will still occur (Cho et al., 2018). Therefore, it is essential to identify the hydrophobicity of insulators promptly through image detection in order to avoid accidents and keep the power system running properly.

And affected by different external factors, the hydrophobic images often have some defects, so that the extraction effect of water droplets in the image is not obvious. In view of this feature, the edge detection algorithm needs to perform certain pre-processing to obtain accurate images for subsequent classification.

To overcome the sensitivity of edge detection algorithms to noise, we incorporate pre-processing steps to reduce noise, which can obscure true edges in insulator hydrophobic images and lead to misdetections or missing critical features. Specifically, Gaussian filtering and median filtering techniques are utilised to smooth the image and suppress noise prior to edge detection. These pre-processing steps help to improve the robustness of the edge detection algorithm against noise, ensuring more accurate and reliable edge detections. Generally speaking, the image manipulation in the edge inspection method of the hydrophobic image is divided into three steps, namely, enhancing the contrast, eliminating the reflection of water droplets, and segmenting the adhering water droplets.

2.1.1 Enhance contrast

In the insulator hydrophobic image, the contrast between the water droplets and the insulator background is very low, which brings great difficulty to the subsequent extraction of water droplets (Pajouhi and Roy, 2018). When performing image processing, the algorithm usually first converts the eal colour figure into a greyscale one, that is, extracts the luminance component for subsequent work, as shown in Figure 1. The procedure for transforming a real colour figure into a greyscale one is to weight proportionally the R, G and B constituent parts of each individual pixel of the real colour figure, and add them together to obtain a two-dimensional image. This conversion method can meet the needs of most image processing, but can not meet the requirements of enhancing the low contrast of hydrophobic images.

Through relevant statistics, it is found that in the insulator hydrophobic image, whether it is a water droplet or a water film, except for the reflective point or reflective area, the R constituent value is almost the same as the surrounding background. However, the value of the G constituent is about 30 lower than the value of the background pixel, and the value of the B constituent is about 40 lower than the value of the background pixel, the R, G, B components of the reflective point are almost close to 240. Whether it is a water droplet or a background pixel, the value of the R constituent is the largest, and the B component is always the smallest. However, when the real colour figure is converted into a greyscale one, the B constituent with the largest difference is assigned the smallest ratio, so the final greyscale image has little contrast, as shown in Figure 2.

Figure 1 Convert colour image to greyscale image (see online version for colours)

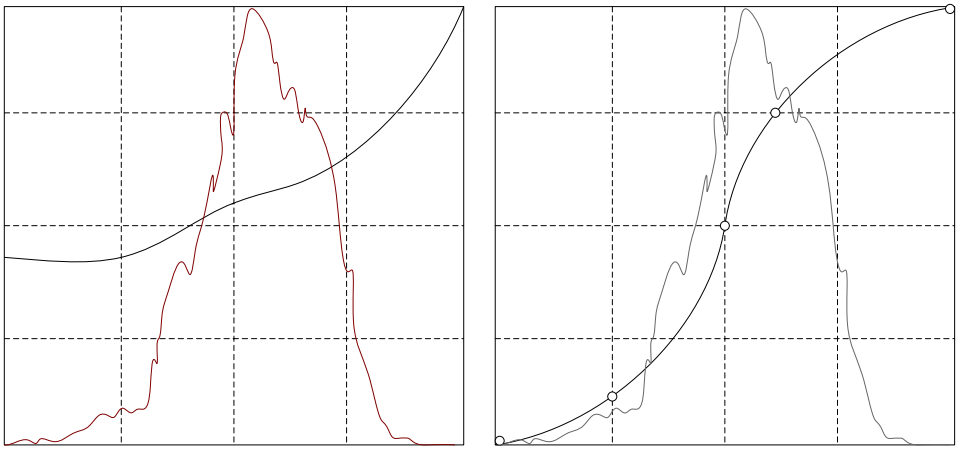

Figure 2 Region blocks with different pixel features (see online version for colours)

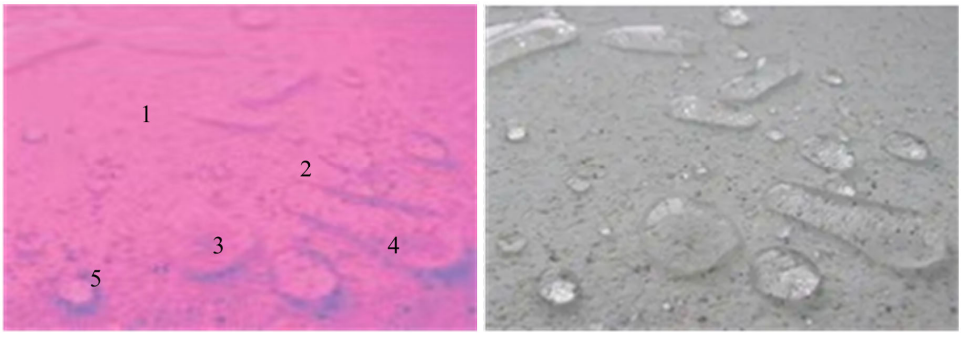

Table 2 Contrast between water drop pixels and background pixels

Pixel count	*Water droplets (R)*	*Background (R)*	*Water droplets (G)*	*Background (G)*	*Water droplets (B)*	*Background (B)*
1	232	237	52	84	3	43
2	235	239	52	83	5	45
3	235	239	51	83	7	45
4	234	237	53	84	6	43
5	236	237	52	83	8	45
6	235	237	51	83	7	45
7	234	238	54	85	8	44
8	234	238	51	84	6	46
9	234	238	51	84	6	46

The places marked with numbers in Figure 2 represent the 5 regions with different pixel characteristics in the hydrophobic image, 1 represents the water film area, 2 represents the reflective area, 3 represents the water drop area, 4 represents the background area, and 5 represents the reflective spot area. Table 2 lists each of the ten pixels in Figure 2.

2.1.2 Eliminate the reflection of water droplets

In insulator hydrophobic image edge detection, the optical properties of water drops and membranes are distinct (Verma and Parihar, 2017). When the water repellency level of the insulator is lower, the water repellency is better, and the more water drops, the greater the contact angle between the water drops and the insulator. At this time, the water droplet is like a convex lens, and under the illumination of strong light, there will be obvious reflection points. This bright spot or bright area is brighter than the surrounding water droplets, and its pixel value components are much larger than other parts of the water droplet, which affects the subsequent extraction of water drops. When the water rejection level of the insulator is high, the water trace gradually becomes a whole water film. At this time, the touch angle separating the water film from the insulator is very small, so there are few or no reflective points. Under normal circumstances, the reflective points or reflective areas of water droplets are treated as uneven illumination. The image edge detection algorithm generally uses histogram equalisation to eliminate the influence of water droplet reflections. When the difference between the brightness of the reflective point or the reflective area and the surrounding pixel value is small, it can play a certain role, but when the difference is large, it basically does not work.

2.1.3 Divide the adhering water droplets

The adhesion of water droplets refers to the slight contact between the edges of two water droplets, which is manifested in the binary image as two white areas are connected by one or two pixels (Duan et al., 2018). In the process of judging the hydrophobicity level of insulators, the image edge inspection method is generally depending on the characteristic value of the largest water droplet or water film in the figure to judge the hydrophobicity. If the sum of the areas of the two adhering water droplets in the figure is greater than the area of the single largest water droplet, the two adhering water droplets will be regarded as one water droplet and their characteristic parameters will be extracted. However, the real largest water droplet is ignored, and errors will occur at this time. For binary images, the narrow connection between two primitives is generally eliminated by morphological opening operation, as described in Figure 3.

For images of water droplets with a large water droplet area and few adhesion parts, the algorithm can meet the requirements. However, for images of water droplets with a small area of water droplets and a large number of adhering parts, the algorithm cannot meet the requirements, the shape of the water droplets will not be accurate enough, and even some water droplets may not be able to be extracted.

2.2 Image edge detection algorithm based on deconvolution deblurring algorithm

While the deconvolution deblurring algorithm exhibits promising results in improving edge detection for insulator hydrophobic images, it is important to note that the method is

computationally intensive and may require significant processing power and time. This can be a challenge for real-time applications in CPS environments. For the purpose of addressing the issues in the edge detection algorithm of insulator hydrophobic image, we adopt a deconvolution deblurring algorithm, efficient optimisation techniques is proposed to improve it, and exploit hardware accelerators such as GPUs to accelerate the computation process. Additionally, we limit the algorithm's complexity by optimising the blur kernel estimation and edge restoration steps, ensuring that the algorithm remains feasible for practical CPS applications.

Figure 3 Open operation process example figure

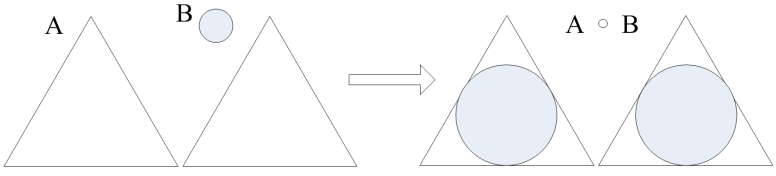

First, model the formation of the insulator hydrophobicity image, and the process is shown in Figure 4.

Figure 4 The process of image formation (see online version for colours)

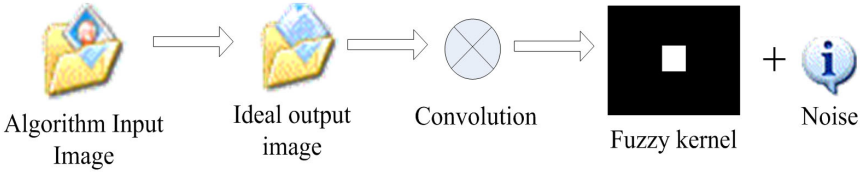

The formula is expressed as:

$$B = I * k + \varepsilon \tag{1}$$

In formula (1), k is the fuzzy core, I is the latent figure, * is the concession operation, ε is the random noise of the figure, and B is the hydrophobic image collected by the imaging system. That is, the hydrophobic image can be regarded as a fuzzy core convolving a clear latent figure, and then adding random noise to get it.

Most of the deconvolution and deblurring algorithms for hydrophobic images mainly take advantage of the property that the sharp edges of hydrophobic images are helpful for kernel estimation when estimating the blur kernel. The algorithm's blur kernel estimation is therefore performed on high-frequency images, that is, one wants to recover the edge ∇I of the insulator hydrophobic image B. The blur kernel estimation can be modelled as formula (2) (Ren et al., 2017):

$$\min_{x,k} \|x * k - y\|_2^2 + \gamma \|k\|_2^2 + \lambda_1 \|x\|_0 \tag{2}$$

Among them, y represents the level and perpendicular gradient of the hydrophobic image $\nabla B = (\partial_x B, \partial_y B)^T$, x represents the level and perpendicular gradient of the clear image $\nabla I = (\partial_x I, \partial_y I)^T$. k stands for the fuzzy kernel, $\|\cdot\|_0$ stands for the l_0 norm, and its function is to calculate the number of non-zero values in x.

Formula (2) contains three terms. The first term is the likelihood term, that is, the convolution of the recovered clear hydrophobic image x and the blur kernel k should be similar to the observed hydrophobic figure y. The latter item is the l_2-norm regularisation item imposed on the blur kernel, which can stabilise the blur kernel estimation. The third term is the l_0-norm regularisation term (Sheng et al., 2020).

The solution of the fuzzy kernel is carried out under a multi-scale solution framework. The solution steps at each scale can be divided into fuzzy kernel estimation and sharp edge recovery, which are expressed as:

$$\min_k \|x * k - y\|_2^2 + \gamma \|k\|_2^2 \tag{3}$$

In the fuzzy kernel estimation stage, the fuzzy kernel can be obtained by formula (3). Since the blur kernel estimation is performed on the high-frequency part of the image, x stands for the level and perpendicular gradient maps of the potentially sharp image, and y stands for the level and perpendicular gradient maps of the blurred image (Chen et al., 2017). The formula is expressed as:

$$x = \nabla I = \begin{pmatrix} \partial_x I \\ \partial_y I \end{pmatrix}, \; y = \nabla B = \begin{pmatrix} \partial_x B \\ \partial_y B \end{pmatrix} \tag{4}$$

Expand the formula to:

$$\min_k \|\partial_x I * k - \partial_x B\|_2^2 + \|\partial_y I * k - \partial_y B\|_2^2 \gamma \|k\|_2^2 \tag{5}$$

In order to simplify the calculation, use FFT to transform the convolution operation in the formula into the multiplication of the corresponding points in the frequency domain, and take the derivative of k, which can be solved to make the formula (5) obtain the minimum value of k, as shown in formula (6).

$$k = f^{-1}\left(\frac{\overline{f(\partial_x I)} f(\partial_x B) + \overline{f(\partial_y I)} f(\partial_y B)}{f(\partial_x I)^2 + f(\partial_y I)^2 + \gamma} \right) \tag{6}$$

In the step of restoring the sharp edge of the hydrophobic image, the term related to k is removed, and formula (7) is obtained:

$$\min_x \|x * k - y\|_2^2 + \|x\|_0 \tag{7}$$

Formula (7) is a non-convex problem with non-differentiable points, which cannot be solved by traditional optimisation methods based on gradient descent, The solution process is very time-consuming if the brute force search method is used (Zhou et al., 2017). The alternating orientation approach is applied here to tackle the problem in formula (7).

Auxiliary variable w is introduced to transform formula (7) into an equivalent problem of formula (8):

$$\min_{x,w} \lambda_1 \|w\|_0 \text{ s.t. } x * k = y, \; w = x \tag{8}$$

Then the Lagrangian function can be obtained as in formula (9), J_1, J_2 represent the Lagrangian multiplier, and u is a penalty parameter:

$$L(x, w, J_1, J_2) = \lambda_1 \|w\|_0 + J_1^T (x - w) + J_2^T (x * k - y) + \frac{u}{2}\left(\|x * k - y\|_2^2 + \|x - w\|_2^2\right) \quad (9)$$

Therefore, the corresponding alternate iteration scheme is:

$$\begin{cases} w^{n+1} = \arg\min_w L\left(x^n, w, J_1^n, J_2^n\right) \\ x^{n+1} = \arg\min_x L\left(x, w^{n+1}, J_1^n, J_2^n\right) \\ J_1^{n+1} = J_1^n + u\left(x^{n+1} - w^{n+1}\right) \\ J_2^{n+1} = J_2^n + u\left(x^{n+1} * k - y\right) \end{cases} \quad (10)$$

The minimum value of $L(x^n, w, J_1^n, J_2^n)$ can be converted to the problem as shown in formula (11):

$$\min_x \left\| x * k + \frac{1}{u} J_2^n - y \right\|_2^2 + \left\| x - w^{n+1} + \frac{1}{u} J_1^n \right\|_2^2 \quad (11)$$

The problem is solved as:

$$\begin{cases} x^n + \dfrac{1}{\mu} J_1^n, & \left(x^n + \dfrac{1}{\mu} J_1^n\right)^2 \geq \dfrac{2\lambda_1}{\mu} \\ 0, & \text{otherwise} \end{cases} \quad (12)$$

Only large-scale hydrophobic image gradient information is beneficial for blur kernel estimation. In the deconvolution image deblurring algorithm, the adaptive weight method is used to enhance the robustness of the blur kernel estimation for hydrophobic images. The large-scale gradient information that has a positive contribution to the blur kernel estimation is screened, and the small image gradient information that has a negative contribution to the blur kernel estimation is removed. The improved model is shown in formula (13) (Shahabinejad and Vosoughi, 2019):

$$\min_{x,k} \|x * k - y\|_2^2 + \gamma \|k\|_2^2 + k\lambda_1 \|x\|_0 \quad (13)$$

Among them, $k = \exp(-|\gamma|^{0.8})$, γ are defined as (Agarwal et al., 2021; Spaic et al., 2020):

$$\gamma = \frac{\left\| \sum_{q \in N_n(p)} \nabla B(q) \right\|_2}{\sum_{q \in N_h(p)} \left\| \nabla B(q) \right\|_2} \quad (14)$$

Among them, B is the insulator hydrophobic image, and $N_n(p)$ is the window of $h * h$ centred on each pixel. For the small-scale edge information, due to the sign of the gradient image $\nabla B(q)$, when calculating $\sum_{q \in N_n(p)} \nabla B(q)$, it will cancel each other out, resulting in γ being too small, so that the small-scale edges that are not conducive to blur kernel estimation can be eliminated.

2.3 Algorithm verification and deconstruction

For the purpose of testing the effectiveness of the edge inspection method of the insulator hydrophobic image considering the deconvolution deblurring algorithm, some standard insulator hydrophobic standard images are tested in this paper, and the image information is shown in Table 3.

Table 3 Basic information of the test image

Sequence	*Size*	*Greyscale*
Hydrophobic image 1	256 × 256	16
Hydrophobic image 2	256 × 256	32
Hydrophobic image 3	512 × 512	32
Hydrophobic image 4	512 × 512	64
Hydrophobic image 5	1,024 × 1,024	32
Hydrophobic image 6	1,024 × 1,024	64

2.3.1 Image detection

In the tests of this paper, in order to examine he implementation of the algorithm under degenerate conditions, the degradation model of the insulator hydrophobic image is used and Gaussian white noise with a standard deviation of 0.5 is added. Firstly, the traditional image edge detection algorithm and the image edge inspection method that takes into account a deconvolution and deblurring method are used to process the insulator hydrophobic degradation image and compare the detection results. The parameters in each algorithm are set to the best value by experimental method. The result is shown in Figure 5.

Figure 5 Hydrophobic image restoration effect under two algorithms, (a) depicts the outcome of the edge detection algorithm in this paper (b) depicts the outcome under the conventional edge inspection algorithm (see online version for colours)

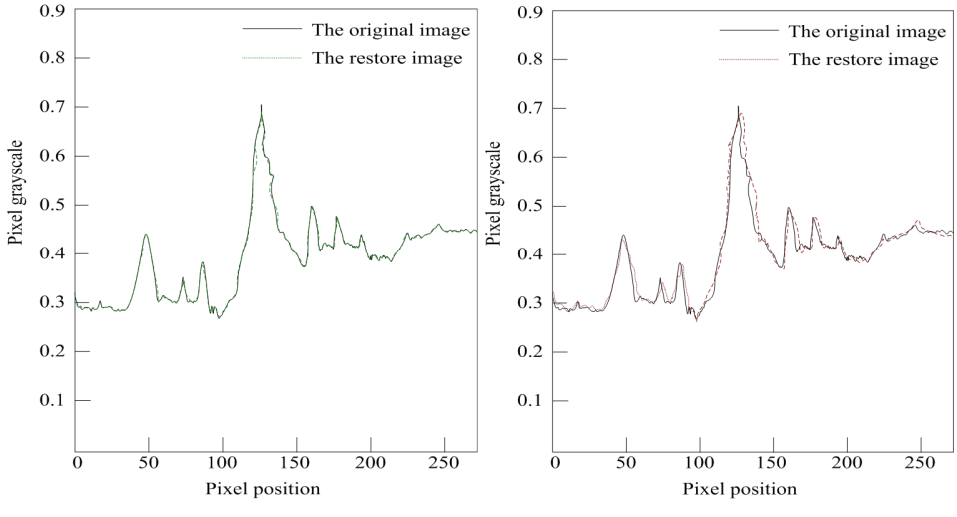

(a) (b)

From the outcome of the edge inspection algorithm in this paper and the conventional approach in Figure 5, it is clear that the insulator hydrophobic image ripple effect in the traditional algorithm is serious, and the edge effect is poor. The reason for this phenomenon is that the establishment of the model in the traditional edge detection algorithm deviates greatly from the original hydrophobic image, which causes the algorithm to deviate from the actual optimum during the iterative procedure. Although the algorithm adjusts for this bias by reconstructing the model, since the new model is based on intermediate estimates, each estimated value is obtained by the same method, which makes it easy to make a certain defect in the image solidify continuously, resulting in more ripples, and the recovery of the edge is difficult to approach the original hydrophobic image.

The edge detecting algorithm suggested in this paper considering the deconvolution deblurring algorithm solves this problem well. After comparison, it is observed that the results of the algorithm in this paper are generally less different from the original hydrophobic images. The outcomes of the algorithm suggested in this paper maintains the better restoration effect of the texture part, has a clearer edge, and also overcomes the problems of image reflection and low contrast in the traditional edge detection algorithm.

2.3.2 Objective assessment

For the purpose of assessing the restoration performance objectively, the peak signal-to-noise ratio (PSNR) and the relative residual error (RRE) are used as evaluation indicators. Although these two evaluation criteria have different forms, they essentially used the discrepancy between the original hydrophobic figure and the estimated hydrophobic figure as the basis for evaluation. The algorithm performance evaluation method used in this experiment is mainly based on these two objective quantitative evaluation standards, supplemented by subjective visual evaluation.

Figure 6 Objective evaluation results of hydrophobic images, (a) shows the PSNR results (b) is the RRE result (see online version for colours)

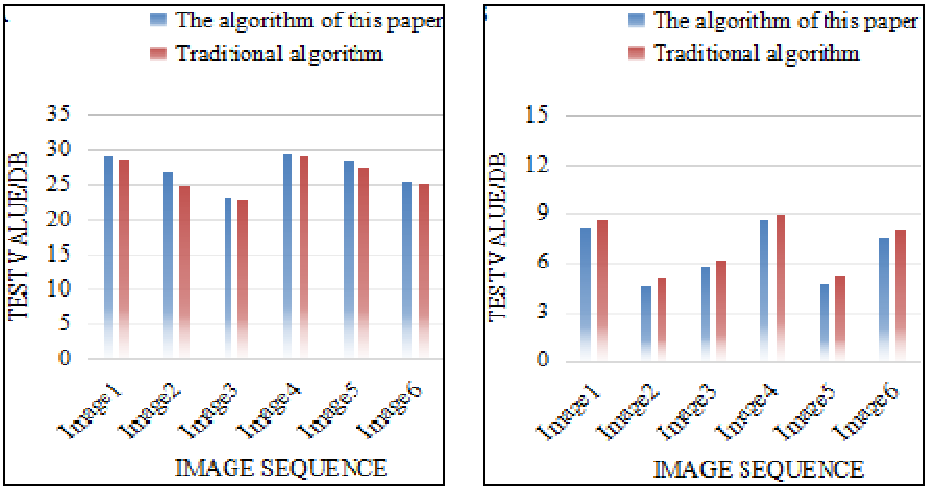

From the objective evaluation metrics in Figure 6, it is apparent that for various test images, the improved edge inspection method in this paper has a superior PSNR ratio than the conventional method. Under the approach in this paper, the comprehensive PSNR ratio of the six types of hydrophobic images is 27.02, while that of the conventional edge inspection method is 26.33, and the improvement range is about 0.3 dB to 1.9 dB. Combined with subjective visual evaluation, it shows that the approach in this paper is valid. In the RRE results, the RRE value of this paper is relatively small, the comprehensive value is only 6.55, while the average RRE value of the traditional edge detection algorithm reaches 6.98. From this result, people can clearly know that the algorithm in this paper has a superior fitting outcome, which makes the resulting image smoother and has a good suppression of noise. However, the traditional insulator hydrophobic edge detection algorithm has been damaged to a certain extent when processing images. The reason is that the images used in the experiments are all natural hydrophobic images. One of the characteristics of natural hydrophobic images is that their pixel greyscale and distribution lack regularity. That is to say, the correlation between them is not strong. In this paper, the modified edge inspection method under the deconvolution deblurring algorithm has strong directionality, so its advantages are well reflected.

2.3.3 Operation time

In terms of operation time, the running time required by the two algorithms to achieve convergence for different hydrophobic images under the degradation model is compared, and the findings are presented in Figure 7.

Figure 7 Algorithm operation time result, (a) shows the operation time of the edge inspection method in this paper (b) shows the operation time of the traditional edge detection method (see online version for colours)

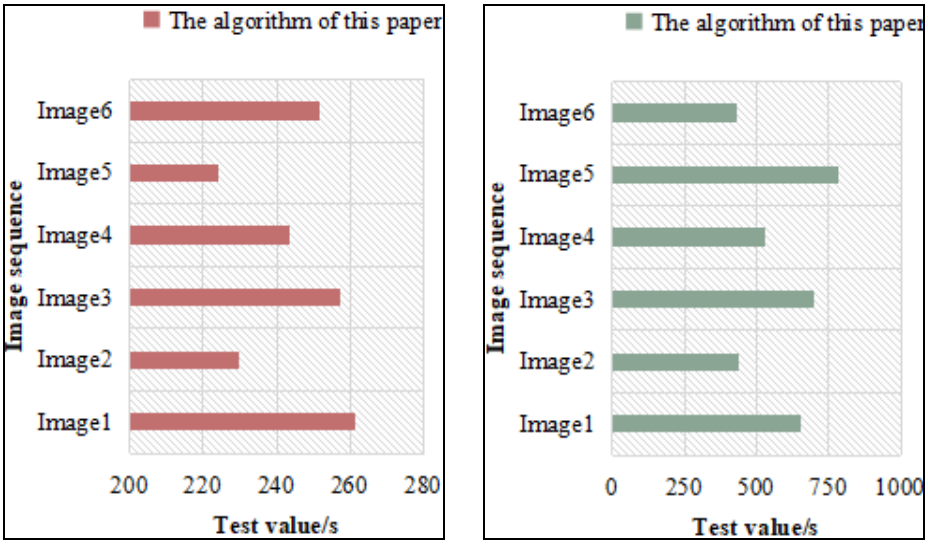

(a) (b)

From the contrast findings of the operation time of the algorithm in Figure 7 in different edge sub-hydrophobic images, it is clear that the present method has an ideal performance on the negative side of the convergence rate. In the face of six types of different hydrophobic images, considering the edge detection algorithm under the deconvolution deblurring algorithm, the comprehensive operation time is 244.53 s. Compared with the traditional edge detection algorithm's comprehensive operation time of 589.77 s, the average operation time of this paper is shortened by about two-thirds. Generally speaking, when edge detection is performed on an insulator hydrophobic image, due to the inherent features of the figure, the algorithm often needs to repeatedly train the model. However, the edge detection algorithm under the deconvolution deblurring algorithm omits this step, which significantly enhances the convergence properties of the algorithm in the edge detection of hydrophobic images, enabling it to output quickly and accurately.

3 Conclusions

The guarantee of insulator performance is inseparable from the safe development of power grid construction. As an important parameter to detect insulator performance, hydrophobicity is particularly critical for its image edge detection algorithm. In this paper, the conventional edge detection method is improved by combining the deconvolution deblurring algorithm. In view of the problems of poor edge detection effect and unsatisfactory image restoration in the original algorithm, adaptive weights are used to strengthen the robustness of the estimation of the fuzzy core of hydrophobic images. In addition, the convergence properties of the algorithm are improved, the operation time can be controlled, and the further development of the practicability and feasibility of the algorithm is realised. Although this paper studies the limitations of the insulator hydrophobic image edge detection algorithm from multiple perspectives, the performance of the proposed edge detection algorithm based on deconvolution deblurring can vary with different insulator hydrophobic images and varying illumination conditions, the verification part of the algorithm still needs to be improved. To address this challenge, we suggest future work on adaptive parameter tuning mechanisms that can automatically adjust algorithm parameters based on the input image characteristics. In the follow-up study, further research will be conducted mainly on the shortcomings of the experimental level and research quality, and the utility of the algorithm will be continuously improved to make it put into practical application faster.

Funding statement

This research study is sponsored by Key Scientific Research Projects of Xi'an Traffic Engineering Institute in 2021 and Xi'an Key Laboratory of Monitoring and Prevention of Railway Roadbed Damage. Thank the project for supporting this article!

References

Agarwal, N., Shrivastava, N. and Pradhan, M.K. (2021) 'Hybrid ANFIS-Rao algorithm for surface roughness modelling and optimization in electrical discharge machining', *Advances in Production Engineering & Management*, Vol. 16, No. 2, pp.145–160.

Chang, C.F., Wu, J.L. and Chen, K.J. (2018) 'A hybrid motion deblurring strategy using patch based edge restoration and bilateral filter', *Journal of Mathematical Imaging and Vision*, Vol. 60, No. 1, pp.1–14.

Chang, C.F., Wu, J.L. and Tsai, T.Y. (2017) 'A single image deblurring algorithm for nonuniform motion blur using uniform defocus map estimation', *Mathematical Problems in Engineering*, No. 3, pp.1–14.

Chen, H., Wang, Q. and Wang, C. (2017) 'Image decomposition-based blind image deconvolution model by employing sparse representation', *IET Image Processing*, Vol. 10, No. 11, pp.908–925.

Cheng, L., Shao, S. and Zhang, S. (2018) 'Research on the long-time operation performance of composite insulator shed hydrophobicity under hydrothermal conditions', *High Voltage*, Vol. 3, No. 1, pp.67–72.

Cho, H., Yoon, H.J. and Jung, J.Y. (2018) 'Image-based crack detection using crack width transform (CWT) algorithm', *IEEE Access*, Vol. 6, No. 1, pp.60100–60114.

Duan, Z., Ning, W. and Fu, J. (2018) 'High precision edge detection algorithm for mechanical parts', *Measurement Science Review*, Vol. 18, No. 2, pp.65–71.

Hang, Y., Zhang, Z. and Guan, Y. (2017) 'An adaptive parameter estimation for guided filter based image deconvolution', *Signal Processing*, Vol. 138, pp.16–26, SEP.

Jayabal, R., Karuppaiyan, V. and Rakesh, K.S. (2019) 'Naive Bayesian classifier for hydrophobicity classification of overhead polymeric insulators using binary image features with ambient light compensation', *High Voltage*, Vol. 4, No. 4, pp.324–332.

Leng, X., Ji, K. and Xing, X. (2017) 'Hybrid bilateral filtering algorithm based on edge detection', *IET Image Processing*, Vol. 10, No. 11, pp.809–816.

Pajouhi, Z. and Roy, K. (2018) 'Image edge detection based on swarm intelligence using memristive networks', *IEEE Transactions on Computer-Aided Design of Integrated Circuits and Systems*, Vol. 37, No. 9, pp.1774–1787.

Ren, D., Zuo, W. and Zhang, D. (2017) 'Partial deconvolution with inaccurate blur kernel', *IEEE Trans Image Process*, Vol. 27, No. 1, pp.511–524.

Shahabinejad, H. and Vosoughi, N. (2019) 'SGSD: a novel sequential gamma-ray spectrum deconvolution algorithm', *Annals of Nuclear Energy*, October, Vol. 132, pp.369–360.

Shaik, M.A., Ramesh, A. and Kumari, Y. (2017) 'The performance analysis of edge detection algorithms for image processing in presence of noise', *International Journal of Computer Science Engineering and Information Technology Research*, Vol. 7, No. 2, pp.1–8.

Sheng, B., Li, P. and Fang, X. (2020) 'Depth-aware motion deblurring using loopy belief propagation', *IEEE Transactions on Circuits and Systems for Video Technology*, Vol. 30, No. 4, pp.955–969.

Spaic, O., Krivokapic, Z. and Kramar, D. (2020) 'Development of family of artificial neural networks for the prediction of cutting tool condition', *Advances in Production Engineering & Management*, Vol. 15, No. 2, pp.164–178.

Tao, Yasheng and Sun (2019) 'Fast-time consecutive confocal image deblurring using spatiotemporal fused regularization', *Applied Optics*, Vol. 58, No. 19, pp.5148–5158.

Verma, O.P. and Parihar, A.S. (2017) 'An optimal fuzzy system for edge detection in color images using bacterial foraging algorithm', *IEEE Transactions on Fuzzy Systems*, Vol. 25, No. 1, pp.114–127.

Yu, X., Zhang, Q. and Yang, X. (2018) 'Influence of non-uniform hydrophobicity distribution on pollution flashover characteristics of composite insulators', *Science, Measurement & Technology*, Vol. 12, No. 8, pp.1009–1014, IET.

Zhang, J. and Zhang, Y. (2019) 'Design and implementation of edge extraction algorithm for digital image', *International Core Journal of Engineering*, Vol. 5, No. 9, pp.105–115.

Zhe, H., Cho, S. and Wang, J. (2018) 'Deblurring low-light images with light streaks', *IEEE Transactions on Pattern Analysis and Machine Intelligence*, Vol. 40, No. 10, pp.2329–2341.

Zheng, H., Ren, L. and Ke, L. (2018) 'Single image fast deblurring algorithm based on hyper-Laplacian model', *IET Image Processing*, Vol. 13, No. 3, pp.483–490.

Zhou, T., Popescu, S.C. and Krause, K. (2017) 'Gold – a novel deconvolution algorithm with optimization for waveform LiDAR processing', *ISPRS Journal of Photogrammetry and Remote Sensing*, July, Vol. 129, pp.131–150.